

Polymorphic relation between cavansite and pentagonite: Genetic implications of oxonium ion in cavansite

Naoya ISHIDA*, Mitsuyoshi KIMATA*, Norimasa NISHIDA**, Tamao HATTA***,
Masahiro SHIMIZU* and Takeshi AKASAKA****

*Earth Evolution Sciences, Graduate School of Life and Environmental Sciences,
The University of Tsukuba, 1-1-1 Tennodai, Tsukuba 305-8572, Japan

**Chemical Analysis Division, Research Facility Center for Science and Technology,
The University of Tsukuba, Tsukuba 305-8577, Japan

***Japan International Research Center for Agricultural Sciences,
Independent Administrative Institute, Tsukuba 305-8686, Japan

****Center for Tsukuba Advanced Research Alliance,
University of Tsukuba, Tsukuba 305-8577, Japan

The chemical compositions of cavansite and pentagonite, in which H₂O contents and vanadium (in an unknown oxidation state) are present, were determined by thermogravimetry-differential thermal analysis (TG-DTA), electron spin resonance (ESR), and electron microprobe analysis (EMPA). Furthermore, the mechanism of dehydration of the minerals and presence of the hydrous species such as H₂O, H₃O⁺, and OH⁻ in the aforementioned minerals have been investigated by TG-DTA, high-temperature X-ray diffraction (HT-XRPD) analysis, Fourier-transform infrared (FTIR) spectroscopy, and single-crystal XRD analysis. The results of TG-DTA and HT-XRD revealed that no reversible transitions occur between cavansite and pentagonite when they are heated in air and that no intermediate amorphous phase exists in these two minerals. Gradual dehydration of cavansite in the temperature range of 225–550 °C was attributed to the removal of both oxonium (H₃O⁺) and hydroxyl ions (OH⁻); the IR absorption bands of cavansite observed at 3186 and 3653 cm⁻¹ were assigned to H₃O⁺ and OH⁻ stretching vibrations, respectively. Moreover, the exact distribution of hydrogens in the crystal structure of the cavansite refined in this study was determined by applying the valence-matching principle; the results showed the existence of H₃O⁺ and OH⁻. Thus, the structural formula of cavansite should be revised to Ca(VO)(Si₄O₁₀)·(H₂O)_{4-2x}(H₃O)_x(OH)_x, in contrast to that of pentagonite, Ca(VO)(Si₄O₁₀)·4H₂O. The changes in the ion product constant of water with temperature and pressure suggest that pentagonite is formed when the hydrothermal fluid is in supercritical condition (>300 °C), while cavansite is formed when the hydrothermal fluid is not in supercritical condition. Thus, cavansite is identified as a low-temperature form and pentagonite as a high-temperature one.

Keywords: Cavansite, Pentagonite, Polymorphic relation, Oxonium ion, Hydroxyl ion

INTRODUCTION

Cavansite and pentagonite, which are rare hydrous vanadium silicate minerals, are known to be dimorphs of Ca(VO)(Si₄O₁₀)·4H₂O (Staples et al., 1973). The crystal structures of these minerals have been characterized from the arrangement of their silicate layer. The cavansite network possesses four- and eight-fold rings, whereas the pentagonite network possesses six-fold rings (Evans, 1973). However, in both these minerals, vanadium exists

in the oxidation states of V⁴⁺ (Staples et al., 1973; Chaurand et al., 2007) or a mixture of V⁴⁺ and V⁵⁺ (Evans, 1973; Powar and Byrappa, 2001).

Thermal analyses performed on cavansite (Phadke and Apte, 1994; Powar and Byrappa, 2001) suggested that all the H₂O molecules present in this mineral are zeolitic. However, it was evident from high-temperature crystal structure refinement (220 °C) that the H₂O molecules released upon heating were not zeolitic (Rinaldi et al., 1975). The H₂O content in cavansite (Phadke and Apte, 1994; Powar and Byrappa, 2001) was not in agreement with the ideal value. Thermal analyses performed on pen-

Table 1. Chemical composition of cavansite and pentagonite

| Oxide (wt%) | Cavansite (N ^a =7) | | Pentagonite (N ^a =10) | | Theoret.** |
|------------------------|-------------------------------|-----------|----------------------------------|-----------|------------|
| | Mean | Deviation | Mean | Deviation | |
| CaO | 12.25 | 0.16 | 12.28 | 0.24 | 12.42 |
| VO ₂ | 18.30 | 0.53 | 19.02 | 1.34 | 18.37 |
| SiO ₂ | 53.61 | 0.77 | 54.02 | 0.87 | 53.25 |
| H ₂ O | 15.95 | - | 16.07 | - | 15.96 |
| Total | 100.11 | 1.03 | 101.39 | 2.22 | 100.00 |
| Cations per 11 oxygens | | | | | |
| Ca ²⁺ | 0.982 | 0.012 | 1.017 | 0.015 | 1.000 |
| V ⁴⁺ | 0.992 | 0.026 | 0.973 | 0.051 | 1.000 |
| Si ⁴⁺ | 4.010 | 0.028 | 3.994 | 0.046 | 4.000 |
| Total | 5.984 | 0.005 | 5.984 | 0.008 | 6.000 |

^a Number of analysis.

** Calculated from the ideal formula Ca(VO)(Si₄O₁₀)·4H₂O.

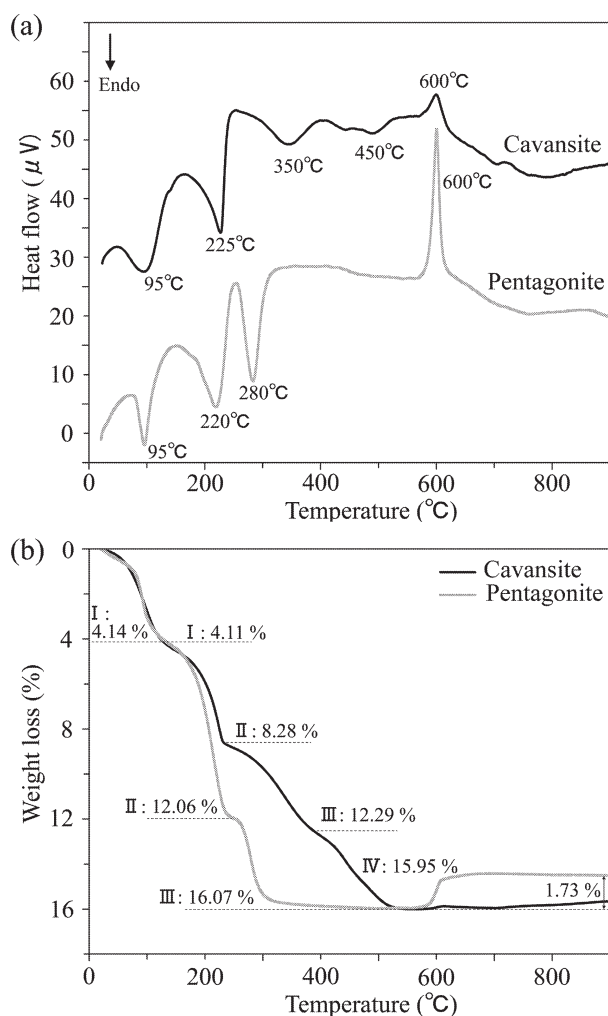


Figure 1. (a) DTA and (b) TG curves obtained for cavansite and pentagonite.

tagonite have not been reported yet.

The identification and roles of hydrous species (H₂O, H₃O⁺, and OH⁻) are unknown in the structures of cavansite and pentagonite (Evans, 1973). A crystal structure refinement of cavansite (Solov'ev et al., 1993) provides un-

usual data for a H₂O molecule: O-H distance of 0.79 Å is too short and H-O-H angle of 81° is too narrow. Meanwhile, there is no information regarding the position of hydrogen atoms in the pentagonite crystal. Many synthetic zeolites such as mordenite (Heeribout et al., 1995), HZSM-5 (Marinkovic et al., 2004), and HSAPO-34 (Smith et al., 1996), have been reported to contain oxonium ions, H₃O⁺, and OH⁻. Recently, it has been proposed that hydrated eudialyte contains H₃O⁺, and this phenomenon is referred to as "oxonium problem" (Rozenberg et al., 2005). Therefore, the analysis of the incorporation of H₃O⁺ into cavansite and pentagonite structures is considered to be very important.

The following are the objectives of this study carried out on cavansite and pentagonite: 1) determination of the oxidation states of vanadium and the H₂O content; 2) identification of the hydrous species in these minerals; and 3) determination of the polymorphic relation between these minerals.

EXPERIMENTAL METHODS

Occurrence and paragenesis

Cavansite and pentagonite used in this study are obtained from Wagholi, India. In Wagholi, these minerals are present in abundance in the cavities of agglomerated breccias coexisting with Deccan basalts (Wilke et al., 1989; Kothavala, 1991; Makki, 2005; Praszkiel and Siuda 2007). The associated minerals of cavansite and pentagonite investigated in the present study consist of mordenite, heulandite, and stilbite, which are commonly observed in this locality (Wilke et al., 1989; Kothavala, 1991; Makki, 2005).

Cavansites resemble rosettes on stilbite or heulandite, and long prismatic crystals of pentagonites grow on stilbite or heulandite. Both cavansite and pentagonite deposits are partially surrounded by a white carpet of extremely fine mordenite needles. Cavansite and pentago-

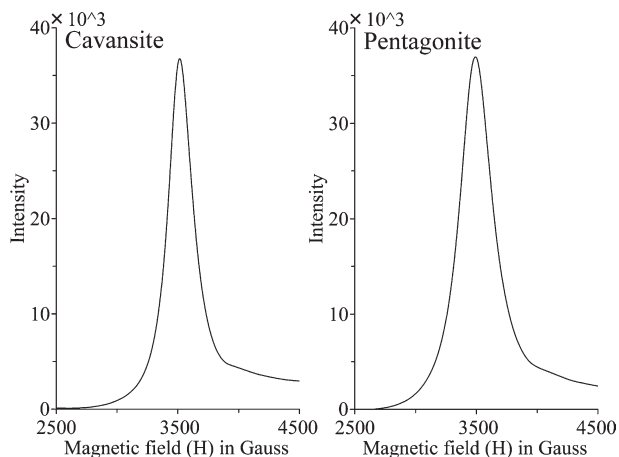


Figure 2. Integrated ESR spectra of cavansite and pentagonite obtained at room temperature.

nite studied herein are not coexistent. Since they have the same associated minerals, the difference in formation mechanism of cavansite and pentagonite has never been debated until now.

Chemical composition

Cavansite and pentagonite were analyzed for identification of the major constituent elements using an electron microprobe analyzer (JEOL JXA-8621) equipped with three wavelength-dispersive spectrometers (Table 1). Quantitative analyses were performed at an accelerating potential of 15 kV and beam current of 10 nA. The standards employed were as follows: wollastonite (Ca), vanadium (V), and quartz (Si). All the data were corrected with a ZAF matrix-correction program. The total H₂O content in cavansite and pentagonite was estimated by thermogravimetry differential thermal analysis (TG-DTA). The detailed experimental procedure is provided in the following section.

TG-DTA

Thermal analyses of cavansite and pentagonite were carried out in air by TG-DTA (Thermo plus TG8120, Rigaku) to clarify the dehydration mechanism, estimate the total H₂O content, and to quantify the amount of reactive oxygen by evaluating the weight gain associated with the oxidation of V⁴⁺ to V⁵⁺ (Fig. 1). Powdered samples of cavansite and pentagonite (~10 mg) were heated in an open platinum crucible at the rate of 10 °C/min up to 900 °C.

Electron spin resonance (ESR) spectroscopy

ESR spectroscopy is used for the analysis of paramagnetic

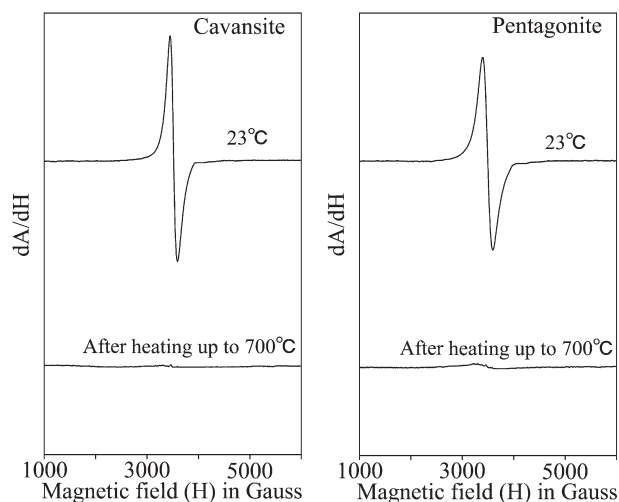


Figure 3. ESR spectra of cavansite and pentagonite obtained at room temperature and after heating to 700 °C.

species. Since V⁵⁺ is diamagnetic and V⁴⁺ paramagnetic, only the latter can be analyzed by ESR (Occhiuzzi et al., 2005). ESR spectroscopy can be effectively used in identifying the oxidation states of vanadium in cavansite and pentagonite. The ESR spectra recorded at room temperature on a Bruker EMX-T spectrometer (X-band) were used to compare the oxidation states of vanadium in cavansite and pentagonite and to confirm the oxidation of V⁴⁺ to V⁵⁺. Each ESR spectrum was measured under the same conditions using 5.0 mg of the powdered sample (Figs. 2 and 3). The magnetic field was swept from 1000 to 6000 G. A blank test was performed to eliminate interference by the background resonance of the cavity.

High-temperature X-ray powder diffraction (HT-XRPD) analysis

HT-XRPD experiments were performed in air with an x-ray diffractometer (RINT-UltimaIII, Rigaku) to identify the products at the temperatures where they were dehydrated or oxidized. CuK α radiation (40 kV, 50 mA) was used as the source. The diffraction patterns were recorded at a scanning rate of 4.0°/min in the 2θ range of 8–50°. The divergence slit width was 1.0 mm, respectively; the scattering slit and light-receiving slit were open, and the opening angle of the long soller slit was 0.114°.

The powdered samples were mounted on platinum plates and heated to 700 °C at the rate of 10 °C/min; the diffraction patterns were recorded at 20, 260, 550, and 700 °C (Figs. 4 and 5). No impurity phases were detected in the XRD patterns. The cavansite and pentagonite samples that were mounted on a non-reflecting quartz plate were cooled after heating up to 400 °C (Fig. 4c) and 550 °C (Fig. 5d), respectively. No peaks corresponding to the

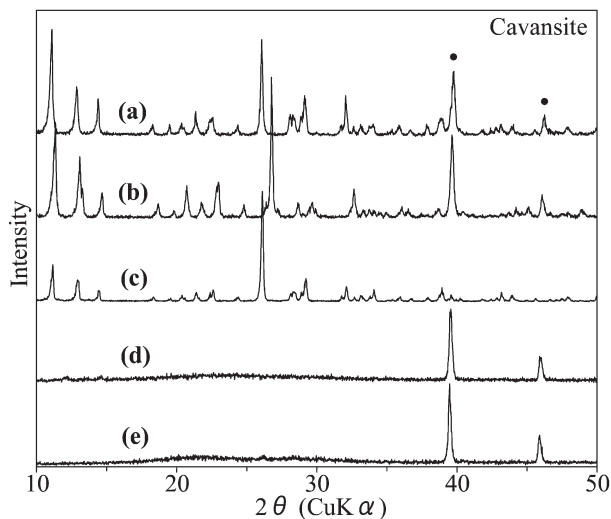


Figure 4. HT-XRPD patterns of cavansite obtained at different temperatures: (a) room temperature, (b) 260 °C, (c) room temperature after heating up to 400 °C, (d) 550 °C, (e) 700 °C. Filled circles correspond to the platinum stage.

platinum phase were observed in the XRD patterns of the samples.

Fourier-transform infrared (FTIR) spectroscopy

Hydrous species present in cavansite and pentagonite were identified using a Janssen-type micro-FTIR spectroscopy (Jasco, Inc.). Single crystals of cavansite and pentagonite (thickness: $\sim 20 \mu\text{m}$) were isolated under a stereomicroscope and placed on a KBr plate. Each spectrum was measured at room temperature between 4000 and 650 cm^{-1} with a resolution of 2 cm^{-1} , and 100 scans were ac-

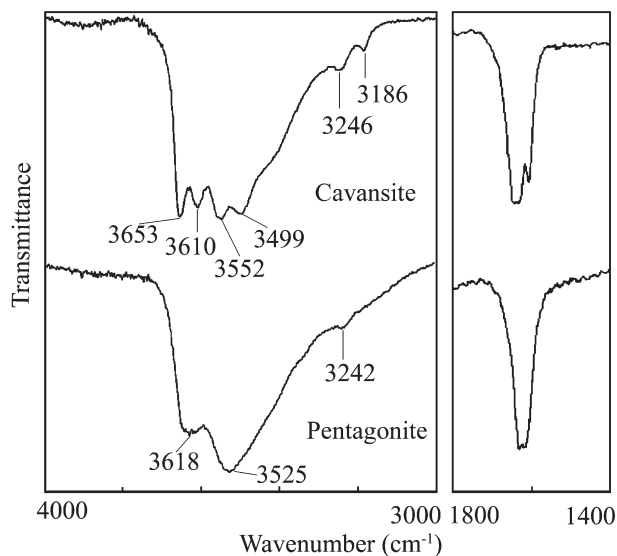


Figure 6. Micro FTIR spectra of a single crystal of cavansite and pentagonite.

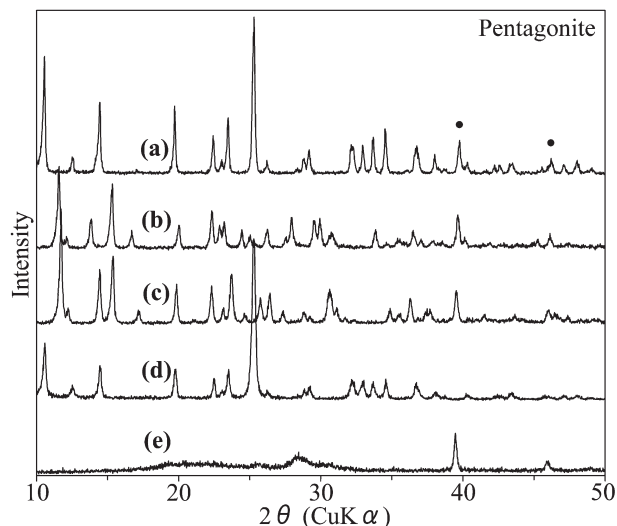


Figure 5. HT-XRPD patterns of pentagonite obtained at different temperatures: (a) room temperature, (b) 260 °C, (c) 550 °C, (d) room temperature after heating up to 550 °C, (e) 700 °C. Filled circles correspond to the platinum stage.

cumulated (Fig. 6).

Single-crystal XRD analysis

Each single crystal of cavansite and pentagonite was fixed on a glass capillary (diameter: 0.1 mm) and mounted on a four-circle diffractometer (Rigaku AFC-7R); the XRD experiments were performed using graphite-monochromatized $\text{MoK}\alpha$ radiation ($\lambda = 0.71069 \text{ \AA}$) as the source. The unit-cell parameters were accurately determined from least-squares fit to the corrected setting angles of 20 reflections in the range of $6^\circ \leq \theta \leq 16^\circ$. Diffraction data were collected at room temperature up to $\theta = 30^\circ$. Using the ψ -scan technique, an empirical absorption correction was applied to the diffraction data. The initial solution of the structure was achieved using direct methods (SIR97: Altomare et al. 1999), and structural refinements were performed using SHELXL-97 (Sheldrick, 1997). Several refinement cycles were carried out using first isotropic, then anisotropic thermal displacement parameters. The final $R1$ values of cavansite and pentagonite converged to 0.034 for 1484 observed reflections [$F_o > 4\sigma(F_o)$] and 0.029 for 1023 observed reflections [$F_o > 4\sigma(F_o)$], respectively. The positions of hydrogen atoms determined by difference Fourier analysis did not match the bond-valence requirements around the oxygen atoms. Therefore, the exact position of hydrogen atoms could not be determined from the crystal structure refinement performed herein. Table 2 summarizes the crystallographic data and the details of the refinements. Tables 3–6 list the atomic coordinates, the atomic displacement parameters, and the

Table 2. Crystal data and refinement details for cavansite and pentagonite

| Mineral name | Cavansite | Pentagonite |
|--|--|-------------------------|
| Chemical formula | Ca(VO)Si ₄ O ₁₀ ·4H ₂ O | |
| Formula weight | 451.45 | |
| Crystal size (mm) | 0.45 × 0.10 × 0.10 | 0.30 × 0.05 × 0.05 |
| Crystal system | Orthorhombic | Orthorhombic |
| Temperature (K) | 298 | 298 |
| Space group | <i>Pcmm</i> | <i>Ccm2₁</i> |
| Z | 4 | 4 |
| <i>a</i> (Å) | 9.794(2) | 10.376(2) |
| <i>b</i> (Å) | 13.670(3) | 14.062(4) |
| <i>c</i> (Å) | 9.643(2) | 8.984(2) |
| <i>V</i> (Å ³) | 1291.1 | 1310.8 |
| <i>F</i> (000) | 876.0 | 876.0 |
| μ (mm ⁻¹) | 1.62 | 1.59 |
| 2 θ_{\max} (°) | 60 | 60 |
| Total reflections | 2914 | 1497 |
| <i>R</i> _{int} | 0.042 | 0.015 |
| Unique reflections | 1955 | 1182 |
| Observed reflections [<i>F</i> _o > 4 σ (<i>F</i> _o)] | 1484 | 1023 |
| Final <i>R</i> 1 [<i>F</i> _o > 4 σ (<i>F</i> _o)] | 0.034 | 0.029 |
| <i>wR</i> 2 | 0.100 | 0.081 |
| Goodness of fit | 1.069 | 1.084 |
| Largest diffraction peak and hole (eÅ ⁻³) | 0.65 and -0.56 | 0.60 and -0.53 |

selected bond distances and angles. Tables 7 and 8 show the results obtained by bond-valence analyses of cavansite and pentagonite; the exact distribution of hydrogens H(1)–H(6) in the refined cavansite and pentagonite structures is confirmed by using the valence-matching principle. Details of the distribution of hydrogens in these minerals are provided in the section titled Hydrus species.

RESULTS AND DISCUSSIONS

Chemical composition

Cavansite and pentagonite have identical chemical compositions within the standard deviation (Table 1). Although back-scattered electron images and X-ray element maps show that each of these crystal grains is chemically homogeneous, it is evident from Table 1 that their chemical compositions involve substantial standard deviations from the theoretical values. The difference could be due to the damage caused to the crystals by the electron beam, which in turn might have caused dehydration of the crystals.

In the present EMPA, we express the vanadium content in cavansite and pentagonite in terms of the VO₂ content. We verify the oxidation states of vanadium as follows. The weight gain (1.73 wt%) observed (from TG-DTA) for pentagonite at 600 °C (Fig. 1b) is approximately equal to the ideal value (1.77 wt%) because of the oxidation of V⁴⁺ to V⁵⁺. ESR data recorded at room temperature show that the integrated peak height corresponding to ca-

vansite is similar to that corresponding to pentagonite (Fig. 2). This indicates that the V⁴⁺ content in cavansite and pentagonite is equal. Therefore, vanadium cations exist only in the +4 oxidation state in cavansite and pentagonite.

Weight change during heating

The TGA curve for cavansite shows four weight loss steps at 95, 225, 350, and 450 °C (Fig. 1a), which correspond to a total weight loss of 15.95 wt% (Fig. 1b); this value is almost equal to the ideal H₂O content (15.96 wt%). The total weight loss of cavansite reported by Phadke and Apte (1994) and Powar and Byrappa (2001) was 13.25 and 13.1 wt%, respectively. The difference in the weight loss reported by the abovementioned researchers is because of the use of impure samples, which contained a contaminant (CuCl phase) and an unidentified phase. Above 600 °C, a gradual weight gain is observed for cavansite (Fig. 1b). This gain is confirmed to be due to the oxidation of V⁴⁺ to V⁵⁺ because no ESR signals are detected in the ESR spectra of the samples heated to 700 °C (Fig. 3). However, the total weight gain in cavansite (~0.4 wt%) is less than the ideal weight gain of reactive oxygen (1.77 wt%). This disagreement is probably because the rate of oxidation of V⁴⁺ to V⁵⁺ is possibly too slow for accurate determination of the proper weight gain; this is because of the oxidation reaction at the heating rate (10 °C/min). Hence, it is concluded that in the case of cavansite, V⁴⁺ is not completely oxidized to V⁵⁺ during the TG-DTA

Table 3. Atomic coordinates and displacement parameters (\AA^2) of cavansite

| Atom | <i>X</i> | <i>y</i> | <i>z</i> | U_{eq} | U_{11} | U_{22} |
|-------|-----------|------------|-----------|-----------------|-----------|-----------|
| Ca | 0.0821(1) | 0.25 | 0.3821(1) | 0.0121(2) | 0.0148(3) | 0.0112(3) |
| V | 0.4035(1) | 0.25 | 0.5259(1) | 0.0100(2) | 0.0120(3) | 0.0094(3) |
| Si(1) | 0.0952(1) | 0.0332(1) | 0.1828(1) | 0.0081(2) | 0.0078(3) | 0.0096(3) |
| Si(2) | 0.3162(1) | 0.0431(1) | 0.3926(1) | 0.0076(2) | 0.0067(3) | 0.0083(3) |
| O(1) | 0.0863(2) | 0.1503(1) | 0.1774(2) | 0.0127(4) | 0.0193(9) | 0.0096(8) |
| O(2) | 0.2937(2) | 0.1577(1) | 0.4123(2) | 0.0127(4) | 0.0157(8) | 0.0074(8) |
| O(3) | 0.4486(2) | 0.0201(1) | 0.2968(2) | 0.0139(4) | 0.0086(9) | 0.0211(9) |
| O(4) | 0.1661(2) | -0.0109(1) | 0.0421(2) | 0.0118(4) | 0.0164(9) | 0.0103(8) |
| O(5) | 0.1855(2) | -0.0045(1) | 0.3141(2) | 0.0111(4) | 0.0118(8) | 0.0113(8) |
| O(6) | 0.5522(3) | 0.25 | 0.4573(3) | 0.0221(6) | 0.018(1) | 0.025(2) |
| O(7) | 0.9460(3) | 0.1183(2) | 0.4708(3) | 0.0418(7) | 0.048(2) | 0.044(2) |
| O(8) | 0.3743(4) | 0.25 | 0.1387(3) | 0.0344(8) | 0.058(2) | 0.031(2) |
| O(9) | 0.8100(5) | 0.25 | 0.2836(5) | 0.0723(2) | 0.057(3) | 0.099(5) |

Table 4. Atomic coordinates and displacement parameters (\AA^2) of pentagonite

| Atom | <i>X</i> | <i>y</i> | <i>z</i> | U_{eq} | U_{11} | U_{22} | U_{33} |
|-------|------------|-----------|-----------|-----------------|-----------|-----------|-----------|
| Ca | 0.2397(1) | 0 | 0.2680(2) | 0.0110(2) | 0.0095(5) | 0.0095(5) | 0.0140(6) |
| V | -0.0223(1) | 0 | 0.0562(1) | 0.0090(2) | 0.0086(4) | 0.0075(4) | 0.0109(5) |
| Si(1) | 0.1275(1) | 0.2060(1) | 0.0882(1) | 0.0073(3) | 0.0064(6) | 0.0073(6) | 0.0082(6) |
| Si(2) | 0.1234(1) | 0.2073(1) | 0.4273(1) | 0.0070(3) | 0.0060(6) | 0.0077(5) | 0.0074(6) |
| O(1) | 0.1216(3) | 0.0926(2) | 0.0838(4) | 0.0121(7) | 0.010(1) | 0.008(2) | 0.018(2) |
| O(2) | 0.1191(3) | 0.0938(2) | 0.4352(4) | 0.0112(7) | 0.012(2) | 0.007(1) | 0.014(2) |
| O(3) | 0.2536(4) | 0.2461(3) | 0.0095(4) | 0.0171(6) | 0.012(1) | 0.019(2) | 0.020(2) |
| O(4) | 0.0034(3) | 0.2546(2) | 0.0062(4) | 0.0127(6) | 0.009(1) | 0.008(1) | 0.022(2) |
| O(5) | 0.1248(3) | 0.2456(2) | 0.2577(5) | 0.0137(6) | 0.021(1) | 0.011(1) | 0.009(1) |
| O(6) | -0.0914(5) | 0 | 0.2136(6) | 0.023(1) | 0.027(3) | 0.027(3) | 0.015(2) |
| O(7) | 0.4003(4) | 0.1173(3) | 0.2381(6) | 0.047(1) | 0.037(2) | 0.051(3) | 0.053(3) |
| O(8) | 0.6196(6) | 0 | 0.0004(8) | 0.053(2) | 0.041(4) | 0.076(6) | 0.041(5) |
| O(9) | 0.3474(9) | 0 | -0.103(2) | 0.131(6) | 0.026(4) | 0.126(10) | 0.24(2) |

experiments.

The three weight loss steps observed at 95, 220, and 280 °C (Fig. 1a) in the TGA curves of pentagonite suggest a total weight loss of 16.07 wt% (Fig. 1b), which is almost equal to the ideal H₂O content (15.96 wt%). The first and third weight loss steps are each ascribable to the release of a H₂O group, whereas the second step is ascribable to the loss of two H₂O groups. The four H₂O groups in pentagonite are classified into three kinds of structural states, and the two H₂O groups released at the second stage may exist in equivalent structural states. At 600 °C, a significant weight gain is observed for pentagonite. This weight gain is thought to be due to the oxidation reaction of vanadium because it is almost identical (1.73 wt%) to the ideal weight gain of reactive oxygen (1.77 wt%).

Structural change during heating

HT-XRPD data for cavansite samples were collected at room temperature and at 260, 550, and 700 °C (Fig. 4). In the present study, HT-XRPD was not carried out at 400 °C (the mean of the third and fourth dehydration temperatures) because of the indistinct transition from the third dehydration stage to the fourth dehydration stage (Fig.

1b). Hence, XRPD experiments were carried out on cavansite samples that were cooled to room temperature after heating up to 400 °C, and the recorded data were examined (Fig. 4c). Lattice parameters for cavansite were obtained for the following three temperature conditions: at room temperature before heating ($a = 9.789(18)$, $b = 13.670(6)$, $c = 9.648(8)$ Å, $V = 1291.0(19)$ Å³), at 260 °C ($a = 9.604(6)$, $b = 13.317(4)$, $c = 9.498(3)$ Å, $V = 1214.7(8)$ Å³), and at room temperature after heating up to 400 °C ($a = 9.782(7)$, $b = 13.654(3)$, $c = 9.632(4)$ Å, $V = 1286.4(8)$ Å³). The close correspondence between the lattice parameters at room temperatures before and after heating to 400 °C indicated that cavansite preserves the original crystal structure and exhibits a thermal behavior similar to that of zeolite. In addition, the diffraction patterns obtained above 550 °C (Figs. 4d and 4e) indicate that above this temperature, cavansite decomposes to amorphous phases; this decomposition occurs after the last dehydration (Fig. 1b). Therefore, the last H₂O group of cavansite is not zeolitic, as predicted by Rinaldi et al. (1975).

HT-XRPD analysis of pentagonite samples is carried out at room temperature and at 260, 550, and 700 °C (Fig. 5). The HT-XRPD patterns observed at 260 and 550 °C

Table 6. Bond lengths (Å) and angles (degree) of pentagonite

| SiO ₄ tetrahedra: | | VO ₅ square pyramids: | |
|------------------------------|----------|----------------------------------|----------|
| Si(1)-O(1) | 1.596(3) | V(1)-O(1)×2 ^d | 1.996(3) |
| Si(1)-O(3) | 1.590(4) | V(1)-O(2)×2 ^{af} | 1.983(3) |
| Si(1)-O(4) | 1.634(3) | V(1)-O(6) | 1.586(5) |
| Si(1)-O(5) | 1.622(4) | | |
| Mean | 1.611 | O(1)-V(1)-O(6) | 103.2(2) |
| | | O(2)-V(1)-O(6) | 105.1(2) |
| O(1)-Si(1)-O(3) | 112.1(2) | O(1)-V(1)-O(2) | 90.8(1) |
| O(1)-Si(1)-O(4) | 112.2(2) | O(1)-V(1)-O(1) | 81.4(2) |
| O(1)-Si(1)-O(5) | 111.5(2) | O(2)-V(1)-O(2) | 83.4(2) |
| O(3)-Si(1)-O(4) | 107.4(2) | | |
| O(3)-Si(1)-O(5) | 108.0(2) | Ca coordination: | |
| O(4)-Si(1)-O(5) | 105.4(2) | Ca(1)-O(1)×2 ^d | 2.437(3) |
| Mean | 109.4 | Ca(1)-O(2)×2 ^d | 2.358(3) |
| | | Ca(1)-O(7)×2 ^d | 2.360(4) |
| Si(2)-O(2) | 1.599(3) | Ca(1)-O(8) ^h | 2.547(6) |
| Si(2)-O(3) ^g | 1.614(4) | Mean | 2.408 |
| Si(2)-O(4) ^c | 1.635(4) | | |
| Si(2)-O(5) | 1.616(4) | | |
| Mean | 1.616 | Possible hydrogen bonds: | |
| | | O(7)-O(3) | 3.13 |
| O(2)-Si(2)-O(3) | 114.0(2) | O(7)-O(4) | 2.96 |
| O(2)-Si(2)-O(4) | 111.4(2) | O(7)-O(5) | 3.03 |
| O(2)-Si(2)-O(5) | 112.0(2) | O(7)-O(8) | 2.88 |
| O(3)-Si(2)-O(4) | 105.9(2) | O(8)-O(9) | 2.97 |
| O(3)-Si(2)-O(5) | 106.8(2) | O(8)-O(2) | 3.07 |
| O(4)-Si(2)-O(5) | 106.3(2) | O(9)-O(1) | 3.17 |
| Mean | 109.4 | O(9)-O(6) | 3.12 |

Notes: Symmetry codes: (a) $-x, y, z-1/2$; (b) $-x+1, y, z-1/2$; (c) $-x, y, z+1/2$; (d) $x, -y, z$; (e) $-x+1/2, -y+1/2, z-1/2$; (f) $-x, -y, z-1/2$; (g) $-x+1/2, -y+1/2, z+1/2$; (h) $-x+1, y, z+1/2$

the IR spectrum of cavansite shift toward a wavenumber higher than that of pentagonite; this shift is characteristic of H₃O⁺ (Marchese et al., 1993).

Analysis of hydrous species on the basis of crystal structure

The refined structural data for the crystals refined in this study were consistent with those reported in the previous studies (Evans, 1973; Solov'ev et al., 1993), except for the characterization of hydrous species. The structures are composed of silicate sheets connected by Ca²⁺ and V⁴⁺ species. A more detailed explanation of the structure is provided in Evans (1973).

The positions of hydrogen atoms in cavansite were determined by Solov'ev et al. (1993); however, a closer

examination of the crystal structure reported by them reveals that the H₂O groups do not satisfy the valence-matching principle (Brown, 1981): (H₂O)₂ was 3.36 valence unit (*vu*) and (H₂O)₃ was 1.64 *vu* in Solov'ev et al. (1993). Hence, the H₂O groups in cavansite must be reexamined on the basis of the bond-valence theory (Brown, 1981). The valence-matching principle (Hawthorne, 1992; Brown, 2002) has been used to analyze the role and types of hydrogen bonding in a crystal (Donnay and Allman, 1970; Hawthorne, 1997; Leclaire et al., 1999; Schindler et al., 2000; Hughes et al., 2002); in this study, this principle is used to study the assignment of hydrogens in the crystal structures of cavansite and pentagonite. The deficiency (2.00 *vu* - 1.64 *vu* = 0.36 *vu*) of O(6) (Table 7) should be compensated by hydrogen bonding; the bond-valence distribution of H(3) to O(6) is 0.33 *vu* and that of H(3) to O(9) is 0.67 *vu*. The remaining bond valence of O(9) (1.33 *vu*) is contributed by H(4) and H(5). The common bond-valence distribution of hydrogen in H₃O⁺ is proposed to be 0.33 *vu* to the further oxygen and 0.67 *vu* to the closer one (Hawthorne, 1997). Therefore, O(9) can partly exist as a H₃O⁺. This assignment is further supported by the eight oxygens coordinated around O(9) in cavansite (Fig. 7) where three short O(9)-O distances (ca. <3.05 Å) that correspond to the hydrogen bonds: one O(9)-O(6) (3.03 Å) and two O(9)-O(7) (2.88 Å). This environment indicates that O(9) has three hydrogen bonds. In pentagonite, there are eight oxygens coordinated around O(9) in pentagonite (Fig. 8) where two O(9)-O distances (~<3.20 Å) that correspond to the hydrogen bonds: one O(9)-O(1) (3.17 Å) and one O(9)-O(6) (3.12 Å). Therefore, O(9) in pentagonite exists as H₂O. Similarly, hydrogen atoms are assigned to the other oxygen atoms; thus, O(7) can partly exist as OH⁻, and O(8) is identified as oxygen in the H₂O groups (Table 6). However, the assignments of hydrogen atoms are not complete because of the possible disordering of hydrogen atoms in the crystal structure of cavansite. An important finding here is that O(7) and O(9) in cavansite are partly substituted for OH⁻ and H₃O⁺, respectively.

Analysis of hydrous species on the basis of thermal behavior

In the TG analysis of cavansite, the third and fourth dehydrations proceeded more slowly than all the other dehydrations in cavansite and pentagonite (Fig. 1b). In HZSM-5, the dehydrations with similar TG curves were thought to correspond to the loss of H₃O⁺ and OH⁻ (Marinkovic et al., 2004). Another observation suggested that the TG curves observed for synthetic alunites of K-H₂O solid solution series showed a gradual slope with an increase in

Table 7. Bond–valence sums for cavansite calculated from the refined bond lengths

| | Ca | V | Si(1) | Si(2) | H(1) | H(2) | H(3) | H(4) | H(5) | ΣV |
|------|---------------------|---------------------|-------|-------|------|---------------------|------|------|------|------|
| O(1) | 0.31 ^{×2↓} | 0.56 ^{×2↓} | 1.06 | | | 0.05 | | | | 1.98 |
| O(2) | 0.28 ^{×2↓} | 0.58 ^{×2↓} | | 1.09 | | 0.05 | | | | 2.00 |
| O(3) | | | 0.99 | 1.00 | | | | | | 1.99 |
| O(4) | | | 0.96 | 0.99 | | | | | | 1.95 |
| O(5) | | | 1.01 | 1.00 | 0.05 | | | | | 2.06 |
| O(6) | | 1.64 | | | | | 0.33 | | | 1.97 |
| O(7) | 0.31 ^{×2↓} | | | | 0.95 | | | 0.33 | 0.33 | 1.92 |
| O(8) | 0.23 | | | | | 0.90 ^{×2→} | | | | 2.03 |
| O(9) | | | | | | | 0.67 | 0.67 | 0.67 | 2.01 |
| ΣV | 2.03 | 3.92 | 4.02 | 4.08 | 1.00 | 1.00 | 1.00 | 1.00 | 1.00 | |

The bond–valence constants are from Brese and O’Keeffe (1991). Bond–valence distributions for hydrogens follow the methods of Hawthorne (1997) and Brown (2002).

Table 8. Bond–valence sums for pentagonite calculated from the refined bond lengths

| | Ca | V | Si(1) | Si(2) | H(1) | H(2) | H(3) | H(4) | H(5) | H(6) | ΣV |
|------|---------------------|---------------------|-------|-------|------|------|------|------|------|------|------|
| O(1) | 0.28 ^{×2↓} | 0.56 ^{×2↓} | 1.08 | | | | | | 0.05 | | 1.97 |
| O(2) | 0.35 ^{×2↓} | 0.58 ^{×2↓} | | 1.07 | | | | | | | 2.00 |
| O(3) | | | 1.10 | 1.03 | | | | | | | 2.13 |
| O(4) | | | 0.97 | 0.97 | 0.20 | | | | | | 2.14 |
| O(5) | | | 1.01 | 1.02 | | 0.10 | | | | | 2.13 |
| O(6) | | 1.71 | | | | | | | | 0.20 | 1.91 |
| O(7) | 0.35 ^{×2↓} | | | | 0.80 | 0.90 | 0.05 | | | | 2.10 |
| O(8) | 0.21 | | | | | | 0.95 | 0.80 | | | 1.96 |
| O(9) | | | | | | | | 0.20 | 0.95 | 0.80 | 1.95 |
| ΣV | 2.17 | 3.99 | 4.16 | 4.09 | 1.00 | 1.00 | 1.00 | 1.00 | 1.00 | 1.00 | |

The bond–valence constants are from Brese and O’Keeffe (1991). Bond–valence distributions for hydrogens follow the methods of Hawthorne (1997) and Brown (2002).

the H₃O⁺ content (Rudolph et al., 2003). Moreover, the last dehydration stage (400–550 °C) in cavansite causes its structure to breakdown, resulting in the formation of the amorphous phase (Fig. 4d). Hence, the hydrous species in cavansite may be identified as H₃O⁺ and/or OH[−]. This identification of hydrous species is consistent with

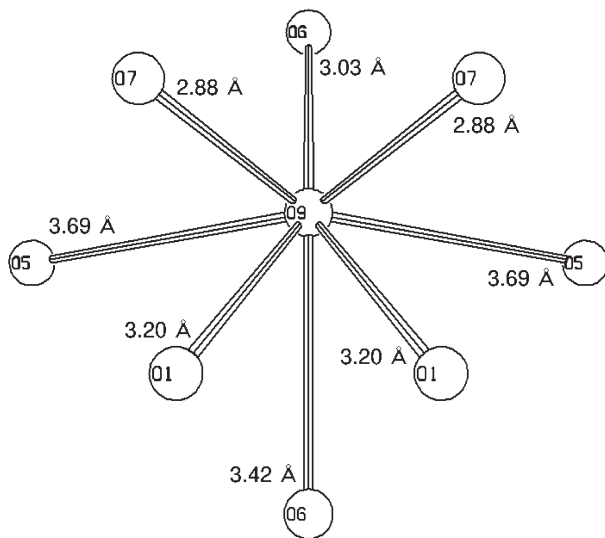


Figure 7. The oxygen coordination environment around O(9) in cavansite.

our earlier result, which states that the last H₂O released when heating cavansite is not zeolitic. Since H₃O⁺ and OH[−] are positively and negatively charged, respectively, the gradual oxidation of V⁴⁺ to V⁵⁺ in cavansite above 600 °C may be attributed to the release of these hydrous species from the crystal structure of cavansite.

The stretching vibration modes of pentagonite that indicate IR absorption bands observed at 3618, 3525, and 3242 cm^{−1} (corresponding to H₂O groups) can be assigned to the H₂O group (Farmer, 1974). Since the three-stage dehydration behavior was clearly observed during the TG analysis of pentagonite (Fig. 1b), all the H₂O groups can be identified to be zeolitic.

Polymorphic relation between cavansite and pentagonite

Chemical analyses of cavansite and pentagonite (Table 1) reveal that both these minerals are polymorphic; however, it has not yet been confirmed that a reversible transformation occurs between them. It is apparent that the polymorphic transition between these minerals will be of a reconstructive type, as is explained by the difference between the network of four- and eight-fold rings with SiO₄ tetrahedra in cavansite and that of six-fold rings in pentagonite (Evans, 1973). As a result, hydrous species (H₂O, H₃O⁺,

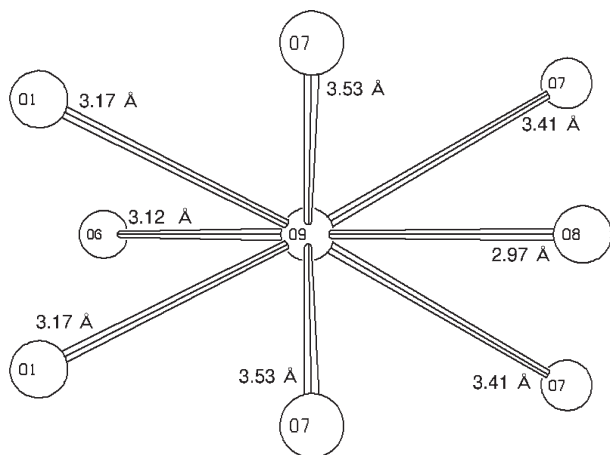


Figure 8. The oxygen coordination environment around O(9) in pentagonite.

and OH⁻) play different roles in the crystal structures of these minerals.

There is a general assumption that in some minerals the following exchange reactions may occur: $\text{H}_3\text{O}^+ + \text{OH}^- \leftrightarrow \text{H}_2\text{O} + \text{H}_2\text{O}$ (Wilkins et al., 1974) or $\text{H}_3\text{O}^+ + \text{OH}^- \leftrightarrow \text{M}^{2+} + \text{O}^{2-}$ (M is a divalent cation) (Sobry, 1971). Since there is neither an excess of H_2O nor a deficiency of Ca^{2+} in cavansite (Table 1), the only possible exchange reaction is $\text{H}_3\text{O}^+ + \text{OH}^- \leftrightarrow \text{H}_2\text{O} + \text{H}_2\text{O}$. Therefore, on the basis of the difference in the roles played by the hydrous species, the chemical formulae of cavansite and pentagonite are determined to be $\text{Ca}(\text{VO})(\text{Si}_4\text{O}_{10}) \cdot (\text{H}_2\text{O})_{4-2x}(\text{H}_3\text{O})_x(\text{OH})_x$ and $\text{Ca}(\text{VO})(\text{Si}_4\text{O}_{10}) \cdot 4\text{H}_2\text{O}$, respectively. The former chemical formula raises a new problem in hydrous materials including $n\text{H}_2\text{O}$. The problem is that hydrous materials including $n\text{H}_2\text{O}$ can be substituted with $(\text{H}_2\text{O})_{n-2x}(\text{H}_3\text{O})_x(\text{OH})_x$.

In aqueous solutions, the product of $[\text{H}_3\text{O}^+]$ and $[\text{OH}^-]$ is defined as the ion product constant of water, K_w , which changes with temperature and pressure (Pitzer, 1982). Figure 7, which has been published by Ikariya (2004) shows the dependence of K_w on temperature and pressure; K_w changes significantly at 10 MPa and 300 °C. This im-

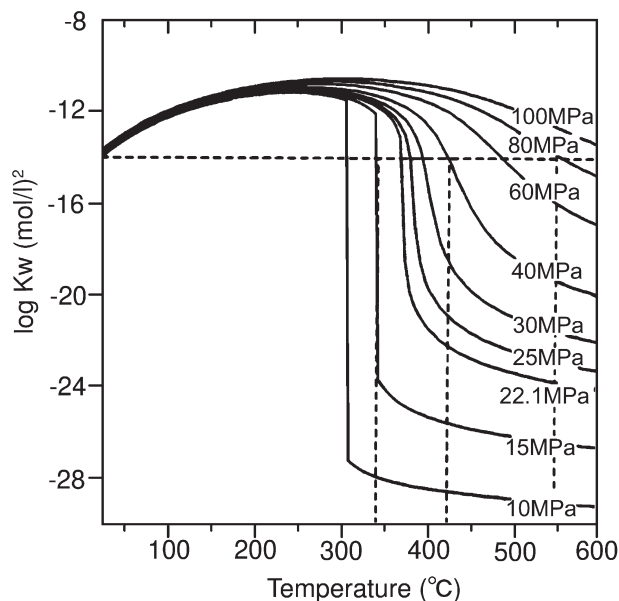


Figure 9. The dependence of K_w [product of (H_3O^+) and (OH^-)] on temperature and pressure (Ikariya, 2004).

plies that the total amount of H_3O^+ and OH^- in aqueous solutions varies dramatically above and below 300 °C. Water above 300 °C at 10 MPa (Fig. 9) which contains neither H_3O^+ nor OH^- is commonly referred to as “supercritical water” (e.g., Franck, 1981). From the structural formula of cavansite proposed in this study, it can be suggested that abundant supply of H_3O^+ and OH^- were afforded by the hydrothermal solution when cavansite was crystallized. On the basis of the changes in K_w with temperature and pressure, it is proposed that the formation of pentagonite or cavansite depends on whether or not the hydrothermal solution is in supercritical condition (above 300 °C). Such a difference in the formation of cavansite and pentagonite cannot be verified by comparing the crystallization temperatures of H_3O^+ -bearing minerals such as jarosite-alunite groups (Ripmeester et al., 1986; Lager et al., 2001), hydrated uranates (Demartin et al., 1991; Chukanov et al., 1999; Chukanov et al., 2004), and clay min-

Table 9. Assignment of hydrogens to the refined oxygens using the difference in bond–valence sum of cavansite

| Solov'ev <i>et al.</i> (1993) | | This study | | |
|---|------|---|-----------------|------------------------------|
| Bond-valence sum for oxygen of water (vu) | | Bond-valence sum for oxygen of hydrous species (vu) | Hydrous species | |
| (H_2O)1–H1...O5 | 2.26 | O(7)–H(1)...O(5) | 1.92 | O(7)H: hydroxyl |
| (H_2O)1–H2...O4 | | Non | | |
| (H_2O)2–H3...O3 | 3.36 | O(8)–H(2)...O(2) | 2.03 | O(8)H ₂ : water |
| (H_2O)2–H3*...O3* | | O(8)–H(2)*...O(1) | | |
| (H_2O)3–H4...O6 | 1.64 | O(9)–H(3)...O(6) | 2.01 | O(9)H ₃ : oxonium |
| (H_2O)3–H5...O6* | | Non | | |
| | | O(9)–H(4)...O(7) | | |
| | | O(9)–H(5)...O(7) | | |

erals (Jiang et al., 1994). However, extensive search on hydrous materials containing H_3O^+ has been carried out in the realm of materials science. A few such materials have been synthesized, such as mordenite (Heeribout et al., 1995), HSAPO-34 zeolite (Smith et al., 1996), HZSM-5 zeolite (Marinkovic et al., 2004), $\text{In}_3(\text{H}_3\text{O})(\text{H}_2\text{PO}_4)_6(\text{HPO}_4)_2 \cdot 4\text{H}_2\text{O}$ (Ivashkevich et al., 2004), $(\text{H}_3\text{O})\text{SbTeO}_6$ (Alonso and Turrillas, 2005), and $\text{NH}_4(\text{H}_3\text{O})\text{Ti}^{\text{III}}\text{Ti}^{\text{IV}}(\text{PO}_4)_3$ (Fu et al., 2005). A careful examination of these synthetic materials reveals that all of them were synthesized below 300 °C, where K_w is large (Fig. 9). These facts are adduced as evidence for the dependence of the stability of hydrous materials on K_w . Therefore, hydrous minerals crystallized below 300 °C must be reexamined for the identification of the hydrous species because they may contain H_3O^+ or perhaps Zundel ions, H_5O_2^+ (Ismael et al., 2005). Cavansite can be regarded as a low-temperature form and pentagonite as a high-temperature one. This is confirmed by the difference in the nature of the tetrahedral ring between the network structures of these two minerals. The cavansite network comprises complex four- and eight-fold rings and the existence of these rings is favored at low temperatures, while the pentagonite network has only six-fold rings of a simple type favorable for the high-temperature environment.

ACKNOWLEDGMENTS

This research is supported by Research Fellowships of the Japan Society for the Promotion of Science for Young Scientists. The authors would like to thank A. Kyono of University of Tsukuba for his continuous advice and critical reading of the manuscript. Furthermore, the authors would like to express their gratitude to M. Hoshino and T. Echigo for their assistance in the crystal structure analysis. The authors are grateful to the Rigaku Corporation for providing the high-temperature X-ray diffractometer, RINT-UltimaIII. The authors would like to thank R. Miyawaki and I. Kusachi for their reviews, which helped improve the manuscript.

REFERENCES

- Alonso, J.A. and Turrillas, X. (2005) Location of H^+ sites in the fast proton-conductor $(\text{H}_3\text{O})\text{SbTeO}_6$ pyrochlore. *Dalton Transactions*, 865–867.
- Altomare, A., Burla, M., Camalli, M., Cascarano, G., Giacovazzo, C., Guagliardi, A., Moliterni, A., Polidori, G. and Spagna, R. (1999) SIR97: a new tool for crystal structure determination and refinement. *Journal of Applied Crystallography*, 32, 115–119.
- Breese, N.E. and O'Keeffe, M. (1991) Bond-valence parameters for solids. *Acta Crystallographica*, B47, 192–197.
- Brown, I.D. (1981) The bond-valence method; and empirical approach to chemical bonding and structure. In *Structure and bonding in crystals* (O'Keeffe, M. and Navrotsky, A. Eds.). New York, Academic Press, 2, 1–30.
- Brown, I.D. (2002) Anion and cation bonding strengths. In *The Chemical Bond in Inorganic Chemistry*. Oxford University Press, New York, 49–50.
- Čejka, J., Sejkora, J. and Deliens, M. (1999) To the infrared spectrum of haynesite, a hydrated uranyl selenite, and its comparison with other uranyl selenites. *Neues Jahrbuch für Mineralogie Monatshefte*, 6, 241–252.
- Chaurand, P., Rose, J., Briois, V., Salome, M., Proux, O., Nassif, V., Olivi, L., Susini, J., Hazemann, J. and Bottero, J. (2007) New methodological approach for the vanadium K-edge X-ray absorption near-edge structure interpretation: application to the speciation of vanadium in oxide phases from steel slag. *Journal of Physical Chemistry B*, 111, 5101–5110.
- Chukanov, N.V., Pekov, I.V., Rastsvetaeva, R.K. and Nekrasov, A.N. (1999) Labunsovite: solid solutions and features of the crystal structure. *The Canadian Mineralogist*, 37, 901–910.
- Chukanov, N.V., Pushcharovsky, D.Y., Pasero, M., Merlino, S., Varinova, A.V., Möckel, S., Pekov, I.V., Zadov, A.E. and Dubinchuk, V.T. (2004) Larisaite, $\text{Na}(\text{H}_3\text{O})(\text{UO}_2)_3(\text{SeO}_3)_2 \cdot 4\text{H}_2\text{O}$, a new uranyl selenite mineral from Repete mine, San Juan County, Utah, U.S.A. *European Journal of Mineralogy*, 16, 367–374.
- Demartin, F., Diella, V., Donzelli, S., Gramaccioli, M. and Pilati, T. (1991) The importance of accurate crystal structure determination of uranium minerals. I. Pohphuranylite $\text{KCa}(\text{H}_3\text{O})_3(\text{UO}_2)_7(\text{PO}_4)_4\text{O}_4 \cdot 8\text{H}_2\text{O}$. *Acta Crystallographica*, B47, 439–446.
- Donnay, G. and Allmann, R. (1970) How to recognize O^{2-} , OH^- , and H_2O in crystal structures determined by X-rays. *American Mineralogist*, 55, 1003–1015.
- Evans, H.T.Jr. (1973) Crystal structures of cavansite and pentagonite. *American Mineralogist*, 58, 412–24.
- Farmer, V.C. (1974) *The infrared Spectra of Minerals*, Mineralogical Society Monograph 4. pp. 165, The Mineralogical Society, London.
- Franck, E.U. (1981) Special aspects of fluid solutions at high pressures and sub- and supercritical temperatures. *Pure and Applied Chemistry*, 53, 1401–1416.
- Fu, Y.L., Xu, Z.W., Ren, J.L. and Ng, S.W. (2005) Langbeinite-type mixed valence $(\text{NH}_4)(\text{H}_3\text{O})\text{Ti}^{\text{III}}\text{Ti}^{\text{IV}}(\text{PO}_4)_3$. *Acta Crystallographica*, E61, 158–159.
- Hawthorne, F.C. (1992) The role of OH and H_2O in oxide and oxysalt minerals. *Zeitschrift für Kristallographie*, 201, 183–206.
- Hawthorne, F.C. (1997) Structural aspects of oxide and oxysalt minerals. *EMU Notes in Mineralogy*, 1, 373–429.
- Heeribout, L., Semmer, V., Batamack, P., Morin, C.D. and Fraissard, J. (1995) Solid-state ^1H NMR Studies of the Acidity of Mordenites. *Journal of the Chemical Society. Faraday Transactions*, 91, 3933–3940.
- Hughes, K.A., Schindler, M., Rakovan, J. and Cureton, F.E. (2002) The crystal structure of hummerite, $\text{KMg}(\text{V}_5\text{O}_{14}) \cdot 8\text{H}_2\text{O}$: bonding between the $[\text{V}_{10}\text{O}_{28}]^{6-}$ structural unit and the $\{\text{K}_2\text{Mg}_2(\text{H}_2\text{O})_{16}\}^{6+}$ interstitial complex. *The Canadian Mineralogist*, 40, 1429–1435.
- Ikariya, T. (2004) Principles and Developments of Supercritical Fluids Reactions. pp. 71, CMC Publishing, Tokyo (in Japanese).
- Ismael, K., Rafael, E., Victor, J.H., Belen, M. and Miguel, A.M.

- (2005): The structure and vibrational frequencies of crystalline HCl trihydrate. *Journal of Molecular Structure*, 742, 147-152.
- Ivashkevich, L.S., Lyakhov, A.S., Selevich, A.F. and Lesnikovich, A.I. (2004): Crystal structure determination of $\text{In}_3(\text{H}_3\text{O})(\text{H}_2\text{PO}_4)_6(\text{HPO}_4)_2 \cdot 4\text{H}_2\text{O}$ from X-ray powder diffraction. *Zeitschrift für Kristallographie*, 219, 543-547.
- Jiang, W.T., Peacor, D.R. and Essene, E.J. (1994): Clay minerals in the MacAdams Sandstone, California: implications for substitution of H_3O^+ and H_2O and metastability of illite. *Clays and Clay Minerals*, 42, 35-45.
- Kothavala, R.Z. (1991): The Wagholi cavansite locality near Poonna, India. *The Mineralogical Record*, 22, 415-420.
- Lager, G.A., Swayze, G.A., Loong, C.K., Rotella, F.J., Richardson, J.W.Jr. and Stoffregen, R.E. (2001): Neutron spectroscopic study of synthetic alunite and oxonium-substituted alunite. *The Canadian Mineralogist*, 39, 1131-1138.
- Leclaire, A., Guesdon, A., Berrah, F., Borel, M.M. and Raveau, B. (1999): Four new Mo(V) phosphate structure built up of isotypic $\text{Mo}_{12}\text{MP}_8\text{X}_{62}$ clusters. *Journal of Solid State Chemistry*, 145, 291-301.
- Makki, M.F. (2005): Collecting cavansite in the Wagholi quarry complex, Pune, Maharashtra, India. *The Mineralogical Record*, 36, 507-512.
- Marchese, L., Chen, J., Wright, P.A. and Thomas, J.M. (1993): Formation of H_3O^+ at the Brønsted Site in SAPO-34 Catalysts. *The Journal of Physical Chemistry*, 97, 8109-8112.
- Marinkovic, B.A., Jardim, P.M., Saavedra, A., Lau, L.Y., Baetz, C., Avillez, R.R. and Rizzo, F. (2004): Negative thermal expansion in hydrated HZSM-5 orthorhombic zeolite. *Microporous and Mesoporous Materials*, 71, 117-124.
- Occhiuzzi, M., Cordischi, D. and Dragone, R. (2005): Reactivity of some vanadium oxides: An EPR and XRD study. *Journal of Solid State Chemistry*, 178, 1551-1558.
- Phadke, A.V. and Apte, A. (1994): Thermal behaviour of cavansite from Wagholi, India. *Mineralogical Magazine*, 58, 501-505.
- Pitzer, K.S. (1982): Self-ionization of water at high temperature and the thermodynamic properties of the ions. *Journal of Physical Chemistry*, 86, 4704-4708.
- Powar, K.B. and Byrappa, K. (2001): X-ray, thermal and infrared studies of cavansite from Wagholi western Maharashtra, India. *Journal of Mineralogical and Petrological Sciences*, 96, 1-6.
- Praszkier, T. and Siuda, R. (2007): The Lonavala Quarry, Pune District, Maharashtra, India. *The Mineralogical Record*, 38, 185-189.
- Rinaldi, R., Pluth, J.J. and Smith, J.V. (1975): Crystal structure of cavansite dehydrated at 220 °C. *Acta Crystallographica*, B31, 1598-1602.
- Ripmeester, J.A., Ratcliffe, C.I., Dutrizac, J.E. and Jambor, J.L. (1986): Hydronium ion in the alunite - jarosite group. *The Canadian Mineralogist*, 24, 435-447.
- Rozenberg, K.A., Rastsvetaeva, R.K. and Khomyakov, A.P. (2005): Decationized and hydrated eudialytes. Oxonium problem. *European Journal of Mineralogy*, 17, 875-882.
- Rudolph, W.W., Mason, R. and Schmidt, P. (2003): Synthetic alunites of the potassium-oxonium solid solution series and some other members of the group: synthesis, thermal and X-ray characterization. *European Journal of Mineralogy*, 15, 913-924.
- Schindler, M., Hawthorne, F.C. and Baur, W.H. (2000): A crystal chemical approach to the structure, chemistry and paragenesis of hydroxy-hydrated oxysalt minerals. I. Theory. *The Canadian Mineralogist*, 38, 1443-1456.
- Sheldrick, G.M. (1997): SHELXL-97. A program for crystal structure refinement. University of Göttingen, Germany.
- Smith, L., Cheetham, A.K., Morris, R.E., Marchese, L., Thomas, J.M., Wright, P.A. and Chen, J. (1996): On the Nature of Water Bound to a Solid Acid Catalyst. *Science*, 271, 799-802.
- Sobry, R. (1971): Water and interlayer oxonium in hydrated uranates. *American Mineralogist*, 56, 1065-1076.
- Solov'ev, M.V., Rastsvetaeva, R.K. and Pushcharovskii, D.Y. (1993): Refined crystal structure of kavansite. *Crystallography Reports*, 38, 274-275.
- Staples, L.W., Evans, H.T.Jr. and Lindsay, J.R. (1973): Cavansite and pentagonite, new dimorphous calcium vanadium silicate minerals from Oregon. *American Mineralogist*, 58, 405-411.
- Wilke, H.J., Schnorrer-Koeler, G. and Bhale, A. (1989): Cavansit aus Indien. *Lapis*, 14, 39-42.
- Wilkins, R.W.T., Mateen, A. and West, G.W. (1974): The spectroscopic study of oxonium ions in minerals. *American Mineralogist*, 59, 811-819.

Manuscript received July 24, 2007

Manuscript accepted March 24, 2009

Published online July 3, 2009

Manuscript handled Tsutomu Sato